### VORTON CONSTRUCTION AND DYNAMICS

Richard A. Battye<sup>1</sup> and Paul M. Sutcliffe<sup>2</sup>

<sup>1</sup> Jodrell Bank Centre for Astrophysics, University of Manchester, Manchester M13 9PL, U.K. Email: Richard.Battye@manchester.ac.uk

<sup>2</sup> Department of Mathematical Sciences, Durham University, Durham DH1 3LE, U.K. Email: p.m.sutcliffe@durham.ac.uk

#### December 2008

#### Abstract

Vortons are closed loops of superconducting cosmic strings carrying current and charge. In this paper we present the first numerical construction of vortons in the global version of Witten's  $U(1) \times U(1)$  theory. An energy minimization procedure is used to compute stationary vortons for a range of charges and currents, and the associated vorton radius is calculated. It is found that the standard analysis based on infinite straight cosmic strings does not provide a good description of the vorton cross-section. The computed solutions are used as initial conditions in an axially symmetric time evolution code, which verifies that the solutions are indeed stationary, and are stable to axially symmetric perturbations. Perturbations which preserve the axial symmetry excite oscillatory modes and produce an evolution which eventually returns to a stationary vorton. Finally, the constructed vorton solutions are used as initial conditions in a full (3+1)-dimensional simulation and an instability to non-axial perturbations is found. The instability produces a pinching and bending of the vorton which results in its destruction.

#### 1 Introduction

Cosmic strings are topological defects which may have formed during a phase transition in the early universe (for a review see [12]). Superconducting cosmic strings were introduced by Witten [13] and possess a non-dissipative current flowing along the string due to the coupling of a second complex scalar field. A closed loop of superconducting string, carrying both current and charge, is known as a vorton [6]. It is a stationary solution in which the current and charge on the string provide a force to balance the string tension and prevent its collapse.

Vortons have a number of potential cosmological consequences [4] and it has been suggested that they may be involved in cosmological phenomena that include galactic magnetic fields, high energy cosmic rays, gamma ray bursts and baryogenesis. It is therefore of considerable interest to determine the stationary properties and dynamical behaviour of vortons.

Despite a number of studies, the existence and stability of vortons as classical field theory solutions is still an open problem, with little convincing evidence, even numerically. Numerical simulations of the relevant nonlinear field theory are difficult to perform in (3+1)-dimensions and results are limited, mainly due to the existence of multiple length and time scales. The problem is also compounded by a large parameter space in which to search. The simplest model expected to have vorton solutions is the global version of Witten's  $U(1) \times U(1)$  theory [13], but even in this theory vorton solutions have not been found. The only field theory computation to date [8] is in a modified version of this theory, in which the interaction term between the two complex scalar fields is replaced by a non-renormalizable interaction, designed to make the numerical problem more tractable. In this modified model a vorton has been presented [8], although even this eventually decays.

In this paper we address the aspects discussed above, by presenting the first numerical construction of vortons in the global version of Witten's  $U(1) \times U(1)$  theory with renormalizable interactions. An energy minimization procedure is used to compute stationary vortons for a range of charges and currents, and the associated vorton radius is calculated. The computed solutions are then used as initial conditions in an axially symmetric time evolution code and this verifies that the solutions are indeed stationary. It is shown that even small axial perturbations of these initial conditions excite reasonably large amplitude long-lived oscillations, though the evolution does produce a slow relaxation back to a stationary vorton. Considerable computational resources are applied to remove the above axially symmetric constraint and perform fully (3+1)-dimensional simulations. These results appear to show that the constructed solutions have an instability to non-axial perturbations. The instability produces a pinching and bending of the vorton which results in its destruction.

Vortons have been analysed in a thin string limit by approximating the loop cross-section by that of an infinite straight cosmic string carrying current and charge [8]. In a planar analogue, known as kinky vortons [3], a similar analysis was found to be in excellent agreement with full numerical simulations of the nonlinear field theory. However, we find that the straight string analysis does not provide a good description of the vortons presented in this paper, and we suggest some reasons for this. Finally, we discuss the relevance of parameter choices for vorton existence and study how the solutions vary as parameters are changed.

## 2 The model and parameters

The Lagrangian density for the global version of Witten's  $U(1) \times U(1)$  model [13] is given by

$$\mathcal{L} = \partial_{\mu}\phi\partial^{\mu}\bar{\phi} + \partial_{\mu}\sigma\partial^{\mu}\bar{\sigma} - \frac{\lambda_{\phi}}{4}(|\phi|^2 - \eta_{\phi}^2)^2 - \frac{\lambda_{\sigma}}{4}(|\sigma|^2 - \eta_{\sigma}^2)^2 - \beta|\phi|^2|\sigma|^2 + \frac{\lambda_{\sigma}}{4}\eta_{\sigma}^4, \tag{2.1}$$

where  $\phi$  and  $\sigma$  are complex scalar fields, with  $\eta_{\phi}, \eta_{\sigma}, \lambda_{\phi}, \lambda_{\sigma}, \beta$  all real positive constants.

The theory has a global  $U(1) \times U(1)$  symmetry and the parameters can be arranged so that in the vacuum the U(1) symmetry associated with  $\phi$  is broken,  $|\phi| = \eta_{\phi} \neq 0$ , while the U(1) symmetry associated with  $\sigma$  remains unbroken,  $\sigma = 0$ . This requires that

$$\lambda_{\phi} \eta_{\phi}^4 > \lambda_{\sigma} \eta_{\sigma}^4. \tag{2.2}$$

For this symmetry breaking pattern there exist global vortex strings constructed from the  $\phi$  field and the interaction term makes it possible that the  $\sigma$  field can form a condensate inside the string core.

One of the difficulties in studying vortons is that the parameter space of the theory (2.1) is quite large and it is not clear which parameter values are compatible with the existence of vortons. Furthermore, one requires vortons that can be computed numerically with reasonable computing resources. This is a significant issue because typically one expects a range of length and time scales to be present in the problem and an accurate numerical resolution could easily require unacceptable resources.

Kinky vortons [3] are (2+1)-dimensional analogues of vortons, in which the role of the cosmic string is replaced by a kink string. In fact the Lagrangian density is precisely the (2+1)-dimensional version of (2.1) with the restriction that  $\phi$  is real. In two space dimensions numerical computations require less resources and also some aspects are more analytically tractable. Studies of kinky vortons suggest that the parameter set

$$\eta_{\phi} = 1, \quad \eta_{\sigma} = 1, \quad \lambda_{\phi} = 3, \quad \lambda_{\sigma} = 2, \quad \beta = 2,$$
(2.3)

may be favourable for the existence of vortons with scales that are feasible for numerical investigation. From now on we restrict to this parameter set, though in Section 5 we shall discuss results for other parameter choices.

A stationary vorton is a solution of the time dependent field equations that follow from (2.1). The  $\phi$  field is static and axially symmetric, describing a circular global string loop. The time dependence of the  $\sigma$  field is in the form of a phase rotation with constant frequency, which induces a non-zero value of the Noether charge Q associated with the unbroken global symmetry

$$Q = \frac{1}{2i} \int (\dot{\sigma}\bar{\sigma} - \dot{\bar{\sigma}}\sigma) d^3x. \tag{2.4}$$

Not only does the vorton carry charge Q but it also carries a current, associated with a phase winding of the  $\sigma$  field along the loop. There is an associated integer N, usually referred to as the winding number, which counts the number of total twists of the phase of  $\sigma$  in a complete

circuit of the loop. Note that although N is traditionally called the winding number and is integer-valued, it is not a topological quantity. It becomes ill-defined if  $\sigma$  vanishes at any point on the circuit around which the winding is defined, and hence can change with time during a continuous time evolution.

String tension will favour a reduction in the radius of a vorton loop but the expectation is that the charge and current in the  $\sigma$  field can provide a force balance that results in a preferred finite non-zero radius. Of course, this will only be the case if the  $\sigma$  condensate remains localized around the string core, and this is far from guaranteed as there is at most a finite energy barrier to be overcome for the two to separate. Analytical and numerical investigations [8] make it clear that a delicate balance between charge Q and winding N (or current) is required, and certainly if either Q or N vanish then there is no vorton solution.

The task is to find suitable values for the quantities Q and N, for which a vorton exists and can be computed, and hence determine its properties, in particular the loop radius. As a vorton solution is not static this can not be achieved using a simple energy minimization approach, but a modification that includes charge conservation can be applied. This is discussed in the following Section and results are presented.

## 3 Vorton construction via energy minimization

For fields that have a time dependence of the form  $\sigma = e^{i\omega t}\psi$ , where  $\psi$  and  $\phi$  are independent of time, the energy can be written as

$$E = \int \left\{ \partial_{i}\phi \partial_{i}\bar{\phi} + \partial_{i}\psi \partial_{i}\bar{\psi} + \frac{\lambda_{\phi}}{4} (|\phi|^{2} - \eta_{\phi}^{2})^{2} + \frac{\lambda_{\sigma}}{4} (|\psi|^{2} - \eta_{\sigma}^{2})^{2} + \beta |\phi|^{2} |\psi|^{2} - \frac{\lambda_{\sigma}}{4} \eta_{\sigma}^{4} \right\} d^{3}x + \frac{Q^{2}}{\int |\psi|^{2} d^{3}x}, \tag{3.1}$$

where we have used the relation

$$Q = \omega \int |\psi|^2 d^3x. \tag{3.2}$$

The fields of a stationary vorton take the axially symmetric form

$$\phi(x, y, z) = \phi(\rho, 0, z), \qquad \psi(x, y, z) = e^{iN\theta} \psi(\rho, 0, z),$$
 (3.3)

where  $\rho$  and  $\theta$  are polar coordinates in the (x,y) plane, so that  $\theta = 0$  corresponds to  $(x,y) = (\rho,0)$ . Without loss of generality, the field  $\psi(\rho,0,z)$  can be chosen to be real.

The fields  $\phi(\rho, 0, z)$  and  $\psi(\rho, 0, z)$  are determined by minimization of the energy (3.1), using a gradient flow algorithm. Rather than solving the problem numerically using cylindrical polar coordinates, the *cartoon* method [1] is employed. This involves using Cartesian coordinates, but restricting the simulations to the slice y = 0. Derivatives are approximated using a second order accurate finite difference scheme with a lattice spacing  $\Delta x$ . To implement the finite difference approximations the fields are also required on the slices  $(x, \pm \Delta x, z)$ , but these are obtained using the axially symmetric ansatz (3.3) by mapping back to the slice

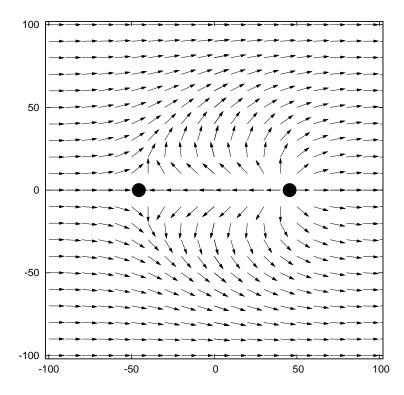


Figure 1: The field  $\phi(x,0,z)$  for a vorton with Q=13000 and N=25, giving a radius R=45.6. The horizontal and vertical length of each arrow is proportional to the real and imaginary parts of  $\phi$ . The black dots denote the points at which  $\phi$  vanishes.

y = 0, and interpolating from the grid in this slice. The *cartoon* method has been successfully used to compute other examples of axially symmetric solitons [7].

In addition to the axial symmetry (3.3) there is also a reflection symmetry

$$\phi(x, y, -z) = \bar{\phi}(x, y, z), \quad \psi(x, y, -z) = \psi(x, y, z),$$
 (3.4)

therefore the computation can be reduced to the quarter plane  $x \geq 0$  and  $z \geq 0$ . The boundary conditions along the symmetry axis  $\rho = 0$  are  $\partial_{\rho}\phi = 0$  and  $\psi = 0$ . Considering the whole plane y = 0, then the vorton configuration has the form of a vortex anti-vortex pair with positions on the positive and negative x-axis. Along a contour at infinity in this plane the winding number of  $\phi$  is zero, and therefore the fields take the constant vacuum values  $\phi = \eta_{\phi}$  and  $\psi = 0$  along this contour. On a finite lattice the computational range is limited to  $-L \leq x \leq L$  and  $-L \leq z \leq L$  and the fields are set to the vacuum values on this computational boundary. Most of the simulations presented here use a lattice spacing  $\Delta x = 0.5$  and have the boundary at L = 100 or L = 200, depending upon the size of the vorton to be computed.

Figure 1 displays the field  $\phi(x,0,z)$ , for a vorton solution with Q=13000 and N=25. The horizontal and vertical components of each arrow are proportional to the real and imaginary parts of  $\phi$ , and this displays the winding properties of the field. The field is constant along the boundary, and hence has zero winding number in the plane. Along the z-axis the field winds exactly once, corresponding to the fact that the winding in the right half plane  $z \geq 0$  is +1 and in the left half plane  $z \leq 0$  is -1. It is important to note that the field is far from the vacuum value over a z range that is of the order of the vorton radius, therefore a thin numerical grid (with less points in the z direction) can not be used, even though this may appear appropriate at first glance.

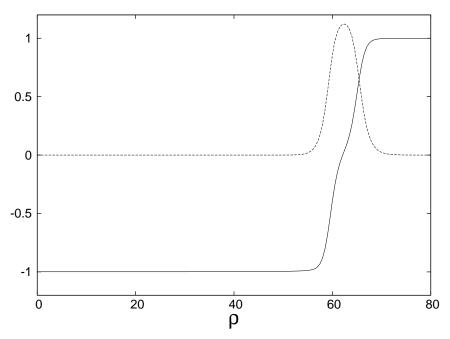


Figure 2: The fields  $\Re(\phi)$  (solid curve) and  $|\sigma|$  (dashed curve) as a function of  $\rho$  in the plane z=0, for a vorton with Q=13000 and N=45, corresponding to R=62.6.

Along the positive x-axis  $\phi$  is real and has a kink-like form, with the vorton radius R defined by  $\phi(R,0,0)=0$ . The values of  $\phi$  and  $|\sigma|$  along this axis are plotted in Figure 2, for the vorton with Q=13000 and N=45, corresponding to R=62.6, and in Figure 3 for the vorton with Q=3000 and N=10, corresponding to R=15.5. Notice that even though the first of these vortons is much larger than the second, the profiles are similar after a translation. This aspect is discussed further in Section 5.

We have been able to construct vorton solutions similar to those presented above for a range of values of Q and N. An illustration of how the vorton properties vary as the physical quantities are changed is provided by Figure 4, which displays the vorton radius R as a function of N for the two values Q = 13000 (circles) and Q = 3000 (squares). In each case there is a limited range of N for which a vorton solution exists, and the width of this range increases with Q. The limited range of N is discussed further in Section 5.

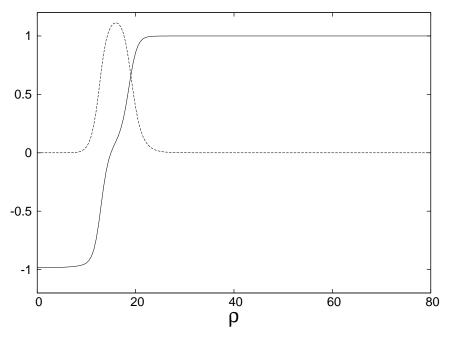


Figure 3: The fields  $\Re(\phi)$  (solid curve) and  $|\sigma|$  (dashed curve) as a function of  $\rho$  in the plane z=0, for a vorton with Q=3000 and N=10, corresponding to R=15.5.

# 4 Dynamics

A good check of the energy minimization results is to use the computed fields as initial conditions in a time evolution simulation and verify that the configuration is indeed stationary. Restricting to axially symmetric fields allows the *cartoon* method to be used.

The time evolution is via an explicit second order accurate finite difference approximation with timestep  $\Delta t = 0.1$ . At the spatial boundary the fields are held at the vacuum values. A small damping term is included, but only on lattice sites which lie within a small distance  $(20\Delta x)$  from the edge of the numerical grid. The role of the damping term is to dissipate any radiation that may be generated without slowing the vorton motion. The frequency  $\omega$  is required as part of the initial conditions but this can be calculated from the energy minimization results using the relation (3.2).

As an example, consider the vorton with Q=3000, N=10, and R=15.5, corresponding to the fields presented in Figure 3. Using the relation (3.2) the frequency is computed to be  $\omega=\omega_*=0.88$ . Figure 5 presents the evolution of the vorton radius R (almost constant dashed line) as a function of time for  $0 \le t \le 5000$ . This confirms the stationary properties of the initial condition produced by the energy minimization computation, to a good accuracy. Similar results have been obtained for other examples.

Next we consider the stability of the constructed vorton solutions by applying a perturbation to the initial conditions. At this stage, the evolution algorithm imposes axial symmetry on the fields so only axially symmetric perturbations can be investigated using the *cartoon* 

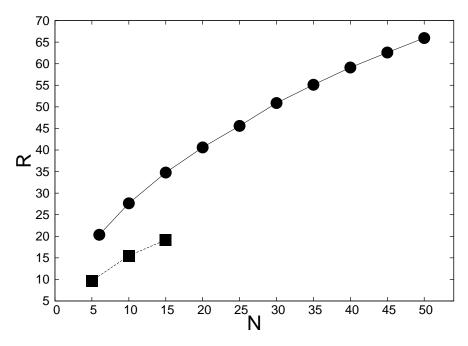


Figure 4: The vorton radius R as a function of winding N, for Q = 13000 (circles) and Q = 3000 (squares). Note the limited range of values of N for which a vorton solution exists.

method. Shortly, we shall address some issues associated with general non-axial dynamics.

The solid curve in Figure 5 corresponds to an evolution where the initial conditions are perturbed through a slight reduction of the initial frequency by 6%:  $\omega=0.94\omega_*=0.83$ . Note that even a small perturbation of this kind produces reasonably large amplitude fluctuations and excites a long-lived oscillatory mode. There is a slow evolution back to a stationary vorton, but of course this is not the original unperturbed vorton because the reduction in the initial frequency means that the initial charge is reduced from Q=3000 to Q=2820. The asymptotic radius that the oscillation approaches is consistent with the radius of the stationary vorton with Q=2820. This result is strong evidence for the stability of this vorton to axially symmetric perturbations, and similar results have been obtained for other examples.

One of the aims of the current work is to find a vorton with reasonable properties that allow a fully (3+1)-dimensional simulation to be performed. In particular, this is required if stability to non-axial perturbations is to be investigated. One condition is that the vorton radius must not be too large in comparison to its width, otherwise the fine grid resolution required to accurately approximate the string cross-section would lead to an unacceptably large number of grid points for a (3+1)-dimensional simulation to incorporate the whole vorton. In particular, this means that the thin string limit, which is mainly used in analytical studies, is beyond current computational feasibility. For (2+1)-dimensional kinky vortons the thin string limit is computationally accessible [3] and the results reveal an excellent

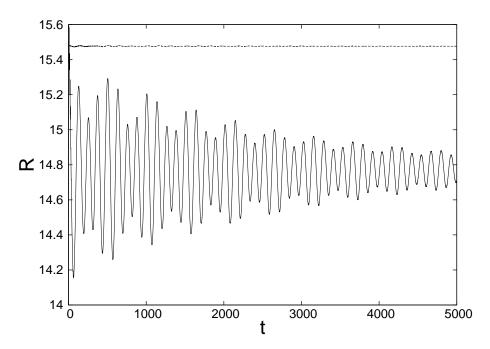


Figure 5: The (almost constant) dashed line is the radius R as a function of time for the evolution of a vorton with Q=3000, N=10, and R=15.5, using the correct frequency  $\omega=0.88$ . The solid curve corresponds to an evolution where the initial conditions are perturbed by a slight reduction of the initial frequency to  $\omega=0.83$ .

agreement with analytical studies.

The vorton presented above with Q=3000, N=10, and R=15.5 appears to be a reasonable candidate for a (3+1)-dimensional simulation. It has a radius which is not much larger than the smallest radius vorton we have been able to find, and it seems a sensible precaution not to choose the smallest possible vorton as this may be a critical case. The axially symmetric energy minimization results can again be used to provide the initial conditions.

An additional complication with (3+1)-dimensional simulations is that the spatial variation of the  $\sigma$  field around the loop, which was treated exactly in the axial case using the ansatz, requires a good resolution. To deal with this issue the lattice spacing used in the axial computations  $\Delta x = 0.5$ , is reduced to  $\Delta x = 0.25$  in the (3+1)-dimensional simulations and, furthermore, the second order accurate spatial finite difference approximations are improved to fourth order accurate versions. Obviously, the reduction in the lattice spacing either requires a corresponding increase in the number of grid points or a reduction in the physical size of the simulation region, or some combination of the two.

The results of a simulation containing  $301^3$  grid points, and therefore  $-L \le x \le L$ , with L = 37.5, are shown in Figure 6. Here the radius R is plotted as a function of time, for the initially unperturbed vorton with Q = 3000, N = 10, and R = 15.5 ( $R/L \approx 0.4$ ). This Figure reveals that the radius oscillates, which at first sight may appear contrary

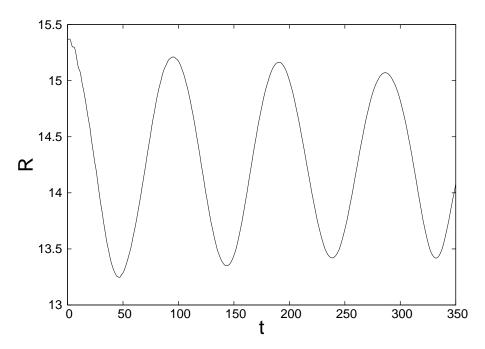


Figure 6: The radius R as a function of time in a fully (3+1)-dimensional simulation of the vorton with Q = 3000 and N = 10.

to expectations since the initial conditions were taken from the energy minimization code. However, the energy minimization algorithm treats the axial dependence of the fields exactly using the ansatz (3.3), and the integration over the polar angle is exact. In contrast, the fully (3+1)-dimensional code only treats the axial dependence approximately and there are discretization errors. This can be seen by computing the charge Q in the (3+1)-dimensional code, where it is found to be Q=2844, which is around 95% of the true value. One therefore expects to see oscillations, with an amplitude similar to that seen in the axial simulation of Figure 5, where a perturbation of the frequency reduced the charge by a similar amount. Figure 6 shows the expected behaviour of a configuration which is close to a stationary vorton and slowly approaching the stationary state.

Figure 7A presents the initial fields and Figure 7B is at the later time t=300 (after 3000 timesteps). In these plots the location and thickness of the vorton is displayed by plotting the red (dark) isosurface  $|\phi|^2 = 0.6$  and the winding number of the  $\sigma$  field is clear from the green (light) isosurface  $\Re(\sigma) = 0.2$ . For this vorton the period for the internal motion is  $T = 2\pi/\omega = 7.14$ , therefore between the first two plots in Figure 7 the vorton has made 42 internal revolutions and has retained its original structure.

The vorton disintegrates shortly after the final time displayed in Figure 6, due to an instability to non-axial perturbations. The cubic boundary, and the fact that it reflects back radiation, provides a small non-axial perturbation that eventually has a clear influence on the vorton, as can be seen by the square deformation in Figure 7C at t=400. As noted above, the boundary is at a distance L=37.5 and this is not substantially larger than the

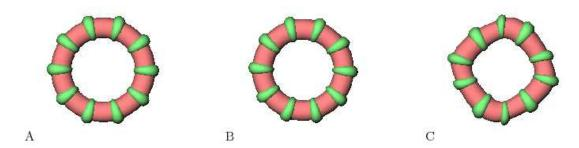


Figure 7: The fields at time (A) t = 0; (B) t = 300; (C) t = 400; for a vorton with Q = 3000 and N = 10. The red (dark) isosurface is where  $|\phi|^2 = 0.6$  and the green (light) isosurface is where  $\Re(\sigma) = 0.2$ 

vorton radius R = 15.5, particularly given the width of the condensate as seen in Figure 3. The non-axial perturbation produces a pinching and bending of the vorton which results in its destruction.

There are several pieces of evidence that support the explanation that the boundary is providing a symmetry breaking perturbation but is not responsible for the instability mechanism, which is physical and not a numerical artifact. One piece of evidence is provided by repeating the above simulation with the same lattice spacing  $\Delta x = 0.25$  but increasing the number of grid points to  $501^3$ , so that the boundary is further away at L = 62.5 ( $R/L \approx 0.25$ ). This produces a very similar result, and in particular the vorton exists for almost the same amount of time.

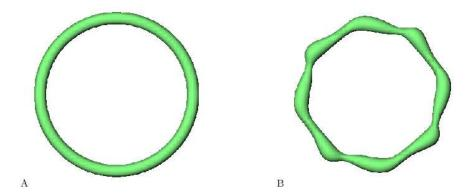


Figure 8: The isosurface  $|\sigma|^2 = 0.5$  at time (A) t = 0; (B) t = 600; for a vorton with Q = 13000 and N = 25. Note the pinching and bending instability excited by the cubic boundary.

Further evidence for the instability is obtained by simulating larger vortons. As an example, consider the vorton displayed in Figure 1 with Q = 13000 and N = 25, giving R = 45.6. This has been simulated using the (3+1)-dimensional code with a lattice spacing

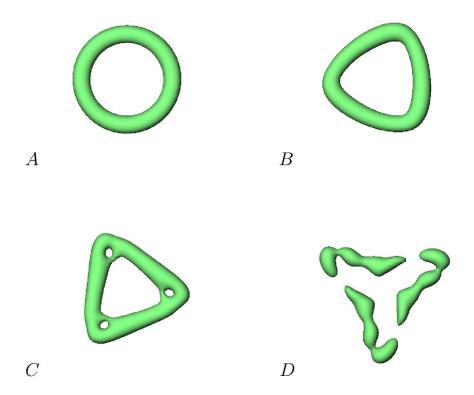


Figure 9: The isosurface  $|\sigma|^2 = 0.4$  at time (A) t = 0; (B) t = 90; (C) t = 120; (D) t = 140; for a vorton with Q = 3000 and N = 10. The vorton has an initial small perturbation with triangular symmetry.

 $\Delta x = 0.5$  and  $301^3$  lattice points, therefore L = 75 ( $R/L \approx 0.6$ ). Figure 8 displays the condensate isosurface  $|\sigma|^2 = 0.5$  at the initial time t = 0 and at the later time t = 600. The perturbation, with square symmetry, induced by the boundary of the grid, is clearly evident together with the pinching and bending modes. Some parts of the vorton cross-section are pinched, while others expand to maintain the total constant charge Q carried by the condensate. Shortly after t = 600 this vorton decays due to this instability.

Finally, perhaps the most convincing evidence is provided by applying a small non-axial perturbation, to dominate over the tiny square perturbation induced by the boundary of the grid. Figure 9 displays the isosurface  $|\sigma|^2 = 0.4$  at increasing times for a vorton with Q = 3000 and N = 10. The vorton has an initial small perturbation with triangular symmetry obtained by scaling the condensate modulus as

$$|\sigma| \mapsto |\sigma|(1 + \varepsilon \sin 3\theta),$$
 (4.1)

where  $\theta$  is the cylindrical polar angle introduced earlier and the amplitude is  $\varepsilon = 0.02$ . The perturbation is small and therefore difficult to detect in the initial condition Figure 9A. However, by t = 90 (Figure 9B) the triangular deformation has grown to a visible amount, and by t = 120 (Figure 9C) the pinching and bending instability is apparent. This Fig-

ure reveals that the bending and pinching combination allows a form of vortex/anti-vortex annihilation to take place and this ultimately destroys the vorton by t=140 (Figure 9D). Note that this perturbation, although small, is easily sufficient to dominate over the tiny square perturbation provided by the boundary. The vorton disintegrates in a much shorter time than with the earlier boundary generated perturbation, and the triangular symmetry is well-preserved, demonstrating that the boundary has a negligible influence in this case.

Studies of both infinite straight strings [8] and (2+1)-dimensional kinky vortons [3] both demonstrate that unstable pinching modes can exist which require breaking the axial symmetry. Similar unstable pinching modes are also found in ferromagnetic vortex rings [11], in certain parameter regimes. Furthermore, unstable non-axial modes can also exist within elastic string models [5]. Numerical studies of elastic string dynamics [9] display bending instabilities, associated with curvature growth, and the qualitative features are remarkably similar to those found in the field theory simulations presented here. It is therefore disappointing, though not surprising, to find unstable modes that involve breaking the axial symmetry.

It appears that all the vortons constructed in this paper have a non-axial instability, but this does not rule out the possibility that other vortons with different values of Q and N, or different parameters of the theory, may be stable. Unfortunately, as mentioned earlier, most regions are not accessible numerically with current computational resources, and indeed it required considerable investigation to find any examples of stationary vortons which are stable even to axially symmetric perturbations.

Note that the vorton simulations presented in the modified model [8] also fail on a time scale that is of a similar order, but it is difficult to know if the reasons are related.

## 5 Infinite string analysis and parameters

One approach to the analysis of vortons is to consider the large radius limit and approximate the vorton cross-section by that of an infinite straight string carrying current and charge [8]. For an infinite string that lies along the z-axis, the appropriate ansatz in cylindrical polar coordinates is

$$\phi = e^{i\theta} |\phi|, \qquad \sigma = e^{i(\omega t + kz)} |\sigma|,$$
 (5.1)

where  $|\phi|$  and  $|\sigma|$  are profile functions that depend only on  $\rho$ . Here k is the rate of twisting and is responsible for the current along the string. It is easy to see that the equations that determine the profile functions depends on k and  $\omega$  only through the combination  $\chi = \omega^2 - k^2$ . In this approach the key aspect is to determine how properties of the profile functions, and also various cross-sectional integrals of these, depend on  $\chi$ . The connection to a vorton loop is then made by identifying the twist rate as k = N/R, where R is the radius of the vorton.

From the form of the ansatz (5.1), it is clear that in terms of the Lagrangian density (2.1) the current and charge together produce a shift by  $\chi$  in the effective mass squared of the  $\sigma$  field. Defining the quadratic coefficients of the two fields by

$$m_{\phi}^2 \equiv \frac{\lambda_{\phi}}{2} \eta_{\phi}^2, \quad m_{\sigma}^2 \equiv \frac{\lambda_{\sigma}}{2} \eta_{\sigma}^2 + \chi,$$
 (5.2)

then the requirement that the U(1) symmetry of the  $\phi$  field is broken and that of the  $\sigma$  field is unbroken yields the constraint [8]

$$\frac{m_{\phi}^4}{\lambda_{\phi}} > \frac{m_{\sigma}^4}{\lambda_{\sigma}}.\tag{5.3}$$

Note that this constraint for infinite straight strings generalizes the earlier constraint (2.2), which is recovered if  $\chi = 0$ . Other constraints can also be obtained, by similar arguments, and this leads to an allowed interval in which  $\chi$  must lie. With the parameters (2.3) used in this paper, the constraint (5.3) imposes the upper bound

$$\chi < \sqrt{\frac{3}{2}} - 1 = 0.22. \tag{5.4}$$

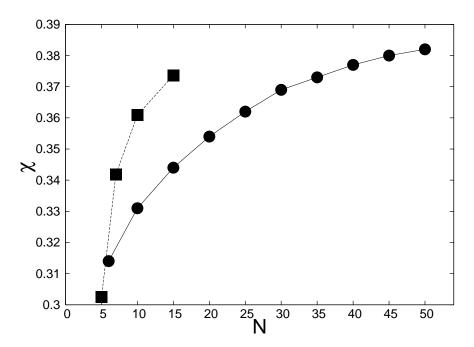


Figure 10:  $\chi$  as a function of N for vortons with Q = 13000 (circles) and Q = 3000 (squares).

Given the numerical results for the vortons constructed using energy minimization then  $\omega$ , N and R are all known for a given vorton and therefore  $\chi = \omega^2 - N^2/R^2$  can be calculated. The results are displayed in Figure 10, where it can be seen that all the obtained values of  $\chi$  violate the infinite string bound (5.4). This is a very surprising revelation and leads to the conclusion that the cross-section of an infinite straight string does not provide a good description of the cross-section of the vortons found in this paper.

Note that  $\chi$  lies in a very small range, suggesting that there is an allowed interval, but it is much higher than that predicted by the straight string analysis. The fact that all

the vortons found have similar values of  $\chi$  also explains the earlier observation that profile functions, such as those displayed in Figure 2 and Figure 3, appear similar after a translation: it is because they have similar values of  $\chi$  and hence similar widths and amplitudes. It is interesting that for different values of Q the allowed range for N seems to correspond to the same range for  $\chi$ , suggesting that there is the same allowed interval for any Q.

We do not have a rigorous explanation of why the straight string analysis appears not to be applicable to these vortons. However, it seems likely that it may be related to the fact that in the global theory a single vortex string has infinite energy per unit length. Only the combination of a vortex/anti-vortex pair has a finite energy, therefore calculating properties based on isolating the vortex and ignoring the anti-vortex is probably not applicable unlike in the local theory. Although kinky vortons are also based on a global theory, in that case a single kink string does have finite energy per unit length, and therefore in this respect behaves more like the local vorton case. The straight string analysis does provide an excellent description for kinky vortons, which supports the idea that the discrepancy is a result of the divergent energy properties of a global vortex, and we believe it is likely that it will also work for local vortons.

Finally, in this section, we briefly mention the results of some investigations using other parameter values in the Lagrangian. Consider a one-parameter family of theories given by

$$\eta_{\phi} = 1, \quad \eta_{\sigma} = 1 + \left(\frac{\sqrt{3}}{2} - 1\right)\mu, \quad \lambda_{\phi} = 3 - \mu, \quad \lambda_{\sigma} = 2, \quad \beta = 2 - \mu.$$
(5.5)

If  $\mu = 0$  then we recover the parameter set (2.3) used throughout this paper, whereas if  $\mu = 1$  then the parameter set is that used extensively in the study of kinky vortons [3].

Using the energy minimization approach we can attempt to compute vortons as  $\mu$  increases away from zero, using  $\mu=0$  vortons as initial conditions, and working piecemeal towards  $\mu=1$ . However, we find that as  $\mu$  increases the solution changes very little until a critical value is reached, which in each case is less than one, where a solution fails to exist. For example, for the vorton with Q=13000 and N=10 the solution exists up to the critical value  $\mu=0.83$ , but for Q=3000 and N=10 the solution only exists up to  $\mu=0.2$ . It, therefore, appears that there are regions in parameter space where solutions for given values of Q and N exist, and this makes the study of vortons particularly difficult. For example, we have not been able to construct any vortons with the parameter set given by  $\mu=1$ , and this is consistent with the piecemeal results, though we have no detailed understanding of this. In fact this is the point where the phase separation condition  $(\beta^2 > \lambda_\phi \lambda_\sigma/4)$  discussed in ref. [2] is violated and this could be part of the explanation. At this stage it appears a very difficult problem to understand and explain the parameter values that will and will not allow vortons.

#### 6 Conclusion

We have used energy minimization methods to compute stationary vortons in the global version of Witten's  $U(1) \times U(1)$  theory and verified that they are stable to axially symmetric perturbations using dynamical simulations. The study of dynamics without axial symmetry reveals that there are unstable modes that are excited by non-axial perturbations. We have also found that an analysis based on infinite straight strings does not seem to provide a good description of the vortons we have computed.

The cosmological and astrophysical applications of vortons require that at least some of the loops formed by the evolution of a cosmic string network survive for a substantial fraction of cosmic time. Our results provide some progress in clarifying this issue, but they do not unequivocally solve the problem. Most importantly, we have found a regime of parameter space where vortons with a radius which can be accommodated in a sensible sized numerical grid can be constructed. We believe that the reason that the infinite string analysis does not yield accurate predictions for the global version of the theory is because of long range interactions associated with a divergence in the energy per unit length. The stability analysis we have performed is far from exhaustive, although we do believe that the independence of the results on R/L suggests that the proximity of the boundary is not the reason for the instability. In the case where the perturbations are created by the cubic symmetry of the numerical grid, the loop is subjected to a wide range of small amplitude modes and it may be that only some of these modes are unstable. Further detailed analysis of the stability properties is clearly needed. It could also be that the very narrow range of  $\chi$  for which solutions can be found plays some role in the apparent sensitivity to perturbations. It would, of course, be of considerable interest to generalize the results in this paper to Witten's original local theory. In particular, we suspect that the failure of the string analysis is due to the properties of a global vortex and therefore the string analysis should be successful in the local theory.

We note that vorton-like stationary solutions have been constructed in a very different regime to those discussed in this paper; and those likely to be relevant to cosmology [10]. In particular, the vorton radius is roughly the same as the string width, so the solutions are as far from the thin string limit as is possible. Furthermore, only solitons with very low winding numbers,  $N \leq 5$ , could be constructed and it was acknowledged that the construction of vortons in the thin ring limit remains a numerical challenge. It would be interesting to see if a connection can be made between these two different regimes of vortons, however, given our earlier results on parameter variations, it seems unlikely that the vortons of one regime will survive all the way to those of a quite different regime. The vortons in [10] were constructed by perturbing away from the sigma model limit  $\lambda_{\phi} = \lambda_{\sigma} \to \infty$  and  $\beta \to \infty$  and it was noted that the solutions are essentially the Skyrmion solutions obtained by the current authors [2] in a related model of a two-component Bose-Einstein condensate. The solutions constructed in the current paper are not well-described by the sigma model approximation: for example, for the solution with Q = 3000 and N = 10 it is found that  $|\phi|^2 + |\sigma|^2$  ranges over the entire interval [0.64, 1.26], and therefore has a substantial variation.

# Acknowledgements

The parallel computations were performed on the Durham University HPC cluster HAMIL-TON, and COSMOS at the National Cosmology Supercomputing Centre in Cambridge. PMS thanks the STFC for support under the rolling grant ST/G000433/1.

#### References

- [1] M. Alcubierre, S. Brandt, B. Brügmann, D. Holz, E. Seidel, R. Takahashi and J. Thornburg, *Int. J. Mod. Phys.* **D10**, 273 (2001).
- [2] R. A. Battye, N. R. Cooper and P. M. Sutcliffe, *Phys. Rev. Lett.* **88**, 080401 (2002); JHEP, PRHEP unesp2002/009 (2002).
- [3] R. A. Battye and P. M. Sutcliffe, Nucl. Phys. **B805**, 287 (2008).
- [4] R. Brandenburger, B. Carter, A. Davis, M. Trodden, Phys. Rev. **D54**, 6059 (1996).
- [5] B. Carter and X. Martin, Annals Phys. 227, 151 (1993).
- [6] R. L. Davis and E. P. S. Shellard, *Phys. Lett.* **B209**, 485 (1988).
- [7] T. Ioannidou and P. M. Sutcliffe, *Physica* **D150**, 120 (2001).
- [8] Y. Lemperiere and E. P. S. Shellard, Nucl. Phys. B649, 511 (2003); Phys. Rev. Lett. 91, 141601 (2003).
- [9] X. Martin and P. Peter, *Phys. Rev.* **D61**, 043510 (2000).
- [10] E. Radu and M. S. Volkov, *Phys. Rep.* **468**, 101 (2008).
- [11] P. M. Sutcliffe, *Phys. Rev.* **B76**, 184439 (2007).
- [12] A. Vilenkin and E. P. S. Shellard, Cosmic Strings and other Topological Defects, Cambridge University Press, 1994.
- [13] E. Witten, Nucl. Phys. **B249**, 557 (1985).